



Study of a time-harmonic load on a Kirchhoff–Love plate with modified thermoelasticity theory using higher-order memory-dependent derivatives

Iqbal Kaur¹ · Kulvinder Singh²

Received: 27 September 2022 / Accepted: 2 June 2023
© The Author(s), under exclusive licence to Springer Nature B.V. 2023

Abstract

In this paper, we study the forced flexural vibrations caused by time-harmonic concentrated loads on a transversely isotropic thin rectangular plate (TRP). A mathematical model has been formed using a new modified Green–Naghdi (GN) III theory of thermoelasticity by introducing higher-order memory-dependent derivatives (MDD). The memory-dependent derivatives represent the memory effect (i.e., the instantaneous rate of change depends on the previous state). This study not only considers the size effect but also studies the memory, mechanical, and thermal-field effects. With the help of the double finite Fourier-transform technique (DFFT), the expressions for lateral deflection, thermoelastic damping, temperature distribution, frequency shift, and thermal moment, have been found in the transformed domain for simply supported (SS) TRP. Also, we have graphically demonstrated the effect of the MDD kernel function on the lateral deflection, thermoelastic damping, temperature distribution, frequency shift, and thermal moment.

Keywords Thin rectangular plate · Memory-dependent derivative · Thermoelastic damping · Lateral deflection · Frequency shift · Thermal moment

Nomenclature

δ_{ij}	Kronecker delta
α_{ij}	Linear thermal expansion coefficient
Ω	Frequency of the applied load
t_{ij}	Stress tensors
c_{ijkl}	Elastic parameters
$\delta()$	Dirac delta function
e_{ij}	Strain tensors
C_E	Specific heat

✉ I. Kaur
bawahanda@gmail.com

K. Singh
ksingh2015@kuk.ac.in

¹ Faculty of Mathematics, Government College for Girls, Palwal, Kurukshetra, India

² Faculty of Engineering, UIET Kurukshetra University, Haryana, India

I	Moment of inertia
T_0	Reference temperature
K_{ij}	Thermal conductivity
w	Transverse displacement
∇^4	Biharmonic operator
T	Absolute temperature
$K(t - \xi)$	Kernel function
u_i	Components of displacement
e_0	Material constant
M_{xx}, M_{yy}	Bending moments
ρ	Medium density
τ_0	Relaxation time
M_{xy}	Twisting moment
β_{ij}	Thermoelastic coupling tensor
β_1	Thermoelastic coupling
M_T	Thermal moment
t	Time
χ	Delay
f_i	Body forces
$q(x, y, t)$	Applied load per unit area
∇^2	Laplacian operator
\vec{u}	Displacement vector
ρ	Density of the material of the plate
a	Internal characteristic length
K_{ij}^*	Material constant

1 Introduction

There are a variety of important and diverse applications for generalized thermoelasticity in recent years, which have caught the attention of many researchers. The fabrication of microchips, as well as many mechanical structures, require elastic thin plates. Size-based continuum mechanics theories are becoming increasingly important with the development of micro- and nanotechnology. There is no doubt that every profession needs to be modified at some point. Therefore, significant and advantageous characteristics and processes can always be improved, as well as mechanical and production processes. A large number of existing models of physical procedures have been changed using fractional calculus over the past several decades, and its applications are employed in many fields including physics, continuum mechanics, and biology. Conversely, when it comes to fractional differential operators, they are not local. Therefore, the current and previous states of the system are used to revise its state.

The Kirchhoff–Love model (Love 1888) of plate deformation and stress in two dimensions is used to investigate how moments and forces influence thin plates. Kirchhoff’s theory is based on Euler–Bernoulli beams and has the following kinematic considerations: (i) during deformation, the thickness of the plate (h) remains constant and is small in comparison to its lateral dimensions; (ii) the central plane of the plate does not exhibit any inplane deformation and remains normal after bending or deforming; (iii) the midsurface displacement’s component amounts are negligible in comparison to the plate thickness; (iv) normal stress,

shear deformation, and strain in the transverse direction can be disregarded. Modern alternatives to fractional-order derivatives are MDDs. Temporal remodeling can be better achieved with MDDs than with FODs. There is a greater demonstration of the memory effect in this case. To explain the memory effect in thermoelasticity, a better MDD model of thermoelasticity was introduced. “MDD is defined in an integral form of a common derivative with a kernel function on a slip-in interval”. Recently, to define the memory dependence, Yu et al. (2014) improved Lord–Shulman (LS) theory by introducing MDD into the rate of heat flux in generalized thermoelasticity theory as $(1 + \chi D_\chi) q_i = -K_{ij} T_{,i}$, ($0 < \chi \leq 1$).

The higher-order Taylor’s series expansion of Fourier’s law that incorporates MDD and kernel functions is presented by Abouelregal et al. (2021a). Abouelregal et al. (2021b) used MD derivatives to develop a new generalized mathematical thermoelastic model consisting of various phase delays and a high-order heat-transfer law. A memory-dependent heat-conduction model with dual phase lags was derived using the modified fractional derivative of Caputo and the higher-order MDD by Abouelregal (2022). Ezzat et al. (2014, 2015, 2016, 2017) discussed the MDD-LS model of generalized thermoelasticity and this was used to solve a few one-dimensional problems. Utilizing the MDD with two temperatures with the modified GN heat-conduction equation, Kaur and Singh (2023) analyzed the fluctuations in a transversely isotropic thick circular plate subjected to ring loading. With the aid of a transversely isotropic, homogeneous plate containing ring loads and two hyperbolic temperatures, Kaur and Singh (2021a) explored fluctuations in fractional-order strain. Kaur and Singh (2021b) investigated the thermoelastic damping in a Kirchhoff–Love plate. Kaur et al. (2020) investigated forced flexural vibrations in a transversely isotropic thermoelastic thin rectangular plate (TRP) using a Kirchhoff–Love plate.

A general model based on Hamilton’s principle was developed by El Kadiri et al. (2002) to describe nonlinear free vibrations of rectangular, homogeneous and composite plates and fully clamped beams at large displacement amplitudes. A nonlinear mechanics theory for shells and plates was developed by Amabili (2008). The vibrations of rectangular plates generated by harmonically excited vibrations of large amplitudes were studied by Amabili (2006). Hamilton’s principle and spectral analysis were used by Beidouri et al. (2006) for the geometric analysis of nonlinear vibrations in thin structures. In a recent study, Majid et al. (2021) examined the impacts of force transverse vibrations on accurately shaped rectangular plates supported by clamped, simply clamped, and simple clamps subjected to significant amplitudes. Other researchers also developed various theories of thermoelasticity, such as Kaur et al. (2020, 2021, 2020), Alzahrani et al. (2020), Trivedi et al. (2022), Sur and Kanoria (2018), Lata et al. (2020), Gupta et al. (2022), Marin et al. (2013), and Kaur and Singh (2021, 2022).

The present investigation focuses on a higher-order memory-dependent derivative (MDD) effect on forced flexural vibrations due to time-harmonic concentrated loads in a TRP. With the DFFT technique, expressions for lateral deflection, thermoelastic damping, temperature distribution, frequency shift, and thermal moment, have been found in the transformed domain for simply supported (SS) TRP. We have demonstrated the effectiveness of the higher-order MDD kernel function on the resultant quantities.

2 Basic equations

2.1 Constitutive equations

A linear elastic solid has the following motion equation according to Kirchhoff (1888):

$$t_{ij,j} + f_i = \rho \ddot{u}_i, \quad (1)$$

$$t_{ij} = c_{ijkl}e_{kl} - \beta_{ij}T, \quad (2)$$

$$e_{ij} = \frac{1}{2}(u_{i,j} + u_{j,i}), \quad i, j = 1, 2, 3, \quad (3)$$

$$\beta_{ij} = c_{ijkl}\alpha_{kl}, \quad (4)$$

where c_{ijkl} ($c_{ijkl} = c_{klij} = c_{jikl} = c_{ijlk}$) are elastic parameters, $\beta_{ij} = \beta_i\delta_{ij}$, $K_{ij} = K_i\delta_{ij}$, $K_{ij}^* = K_i^*\delta_{ij}$, i is not summed,

2.2 Heat-conduction equation

Using Green and Naghdi (1992) and Bachher (2019), the constitutive equation for ATM with GN-III theory with higher-order memory-dependent derivatives is:

$$K_{ij}^*T_{,ij} + K_{ij}\dot{T}_{,ij} = \left(1 + \sum_{r=1}^N \frac{\chi^r}{r!} D_{\chi}^r\right) (\beta_{ij}T_0\ddot{e}_{ij} + \rho C_E\ddot{T}), \quad (5)$$

where the r th-order MDD for a differentiable function $f(t)$ with delay $\chi > 0$ for a fixed time t presented by Wang and Li (2011) is:

$$D_{\chi}^r f(t) = \frac{1}{\chi} \int_{t-\chi}^t K(t-\xi) f^{(r)}(\xi) d\xi. \quad (6)$$

The $K(t-\xi)$ and χ is determined from the material properties. From Ezzat et al. (2014, 2015, 2016) the following kernel function $K(t-\xi)$ is used

$$K(t-\xi) = 1 - \frac{2\beta}{\chi}(t-\xi) + \frac{\alpha^2}{\chi^2}(t-\xi)^2 = \begin{cases} 1 & \alpha = 0, \beta = 0, \\ 1 + (\xi-t)/\chi & \alpha = 0, \beta = 1/2, \\ \xi-t+1 & \alpha = 0, \beta = \chi/2, \\ [1 + (\xi-t)/\chi]^2 & \alpha = 1, \beta = 1, \end{cases} \quad (7)$$

where α and β are constants. Additionally, the comma indicates the derivative w. r. t. the space variable and the dot superimposed on it signifies the time derivative.

3 Method and formulation of the problem

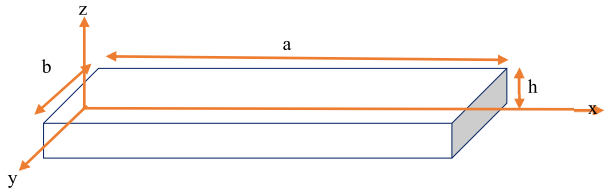
3.1 Formulation

Consider a homogeneous, transversely isotropic thermoelastic thin rectangular plate TRP (Fig. 1) with Cartesian axes (x, y, z) having length a ($0 \leq x \leq a$), width b ($-\frac{b}{2} \leq y \leq \frac{b}{2}$) and thickness h ($-\frac{h}{2} \leq z \leq \frac{h}{2}$). A right-handed set is formed by placing the midsurface of the TRP in the x - y plane and the z -axis toward the thickness direction. The origin is chosen to be at one corner of the center surface of the plate in the chosen coordinate system, as shown in Fig. 1.

The Kirchhoff-Love plate theory is consistent with the deformation of the TRP. Rao (2007) provides the displacement components for a minor deflection of a straightforward bending problem using the fundamental classical theory of a thin plate.

$$u_1(x, y, z, t) = -z \frac{\partial w}{\partial x}, u_2(x, y, z, t) = -z \frac{\partial w}{\partial y}, u_3(x, y, z, t) = w(x, y, t). \quad (8)$$

Fig. 1 Schematic design of the TRP



The TRP's normal and shear strain components are

$$e_{xx} = -z \frac{\partial^2 w}{\partial x^2}, \tag{9}$$

$$e_{yy} = -z \frac{\partial^2 w}{\partial y^2}, \tag{10}$$

$$e_{xy} = -2z \frac{\partial^2 w}{\partial x \partial y}, \tag{11}$$

$$e_{zz} = e_{yz} = e_{xz} = 0. \tag{12}$$

According to Eringen theory, with the use of equation (8), the constitutive equation derived from equation (2) becomes

$$t_{xx} = c_{11} \left(-z \frac{\partial^2 w}{\partial x^2} \right) + c_{12} \left(-z \frac{\partial^2 w}{\partial y^2} \right) - \beta_1 T, \tag{13}$$

$$t_{yy} = c_{12} \left(-z \frac{\partial^2 w}{\partial x^2} \right) + c_{11} \left(-z \frac{\partial^2 w}{\partial y^2} \right) - \beta_1 T, \tag{14}$$

$$t_{xy} = (c_{11} - c_{12}) \frac{1}{2} \left(-2z \frac{\partial^2 w}{\partial x \partial y} \right), \tag{15}$$

$$t_{yz} = t_{xz} = 0, \tag{16}$$

where $\beta_1 = (c_{11} + c_{13})\alpha_1 + C_{13}\alpha_3$.

As per Rao (2007), the M_{xx} , M_{yy} , and M_{xy} are given by

$$M_{xx}(x, y, t) = \int_{-\frac{h}{2}}^{\frac{h}{2}} t_{xx} z dz, \tag{17}$$

$$M_{yy}(x, y, t) = \int_{-\frac{h}{2}}^{\frac{h}{2}} t_{yy} z dz, \tag{18}$$

$$M_{xy}(x, y, t) = \int_{-\frac{h}{2}}^{\frac{h}{2}} t_{xy} z dz. \tag{19}$$

After multiplication of (13)–(15) by z , integration w.r.t z , and with the help of equations (17)–(19) yields

$$M_{xx} = -c_{11} \left(I \frac{\partial^2 w}{\partial x^2} \right) - c_{12} \left(I \frac{\partial^2 w}{\partial y^2} \right) - M_T, \tag{20}$$

$$M_{yy} = -c_{12} \left(I \frac{\partial^2 w}{\partial x^2} \right) - c_{11} \left(I \frac{\partial^2 w}{\partial y^2} \right) - M_T, \quad (21)$$

$$M_{xy} = (c_{11} - c_{12}) \left(-I \frac{\partial^2 w}{\partial x \partial y} \right), \quad (22)$$

where

$$M_T(x, y, t) = \beta_1 \int_{-\frac{h}{2}}^{\frac{h}{2}} T z dz, \quad (23)$$

$$I = \frac{h^3}{12}. \quad (24)$$

According to Rao (2007), Ventsel and Krauthammer (2002), the transverse equation of motion with forced vibrations of the TRP is written as

$$\frac{\partial^2 M_{xx}}{\partial x^2} + 2 \frac{\partial^2 M_{xy}}{\partial x \partial y} + \frac{\partial^2 M_{yy}}{\partial y^2} + q(x, y, t) = \rho h \frac{\partial^2 w}{\partial t^2}. \quad (25)$$

It is assumed that inside the plate at a point (ε, μ) , a time-harmonic concentrated load is applied such that

$$q(x, y, t) = P \delta_\varepsilon(x) \delta_\mu(y) e^{i\omega t},$$

where P is a constant.

Equation (25) with the help of (20)–(24) becomes

$$\begin{aligned} c_{11} I \left(\frac{\partial^4 w}{\partial x^4} + \frac{\partial^4 w}{\partial y^4} + 2 \frac{\partial^4 w}{\partial x^2 \partial y^2} \right) + \left(\frac{\partial^2 M_T}{\partial x^2} + \frac{\partial^2 M_T}{\partial y^2} \right) + \rho h \frac{\partial^2}{\partial t^2} (w) \\ = -P \delta_\varepsilon(x) \delta_\mu(y) e^{i\omega t}. \end{aligned} \quad (26)$$

Therefore, using (8), equation (5) becomes

$$\begin{aligned} \left(K_1^* + K_1 \frac{\partial}{\partial t} \right) \left(\frac{\partial^2 T}{\partial x^2} + \frac{\partial^2 T}{\partial y^2} \right) + \left(K_3^* + K_3 \frac{\partial}{\partial t} \right) \frac{\partial^2 T}{\partial z^2} \\ = \left(1 + \sum_{r=1}^N \frac{X^r}{r!} D_x^r \right) \left(\beta_1 T_0 \frac{\partial^2}{\partial t^2} \left(-2z \left(\frac{\partial^2 w}{\partial x^2} + \frac{\partial^2 w}{\partial y^2} \right) \right) + \rho C_E \ddot{T} \right). \end{aligned} \quad (27)$$

The following dimensionless quantities (DQ) are presented in order to simplify the solution:

$$\begin{aligned} x' = \frac{x}{L}, t'_{xx} = \frac{t_{xx}}{c_{11}}, y' = \frac{y}{L}, t' = \frac{c_1 t}{L}, z' = \frac{z}{L}, w' = \frac{w}{L}, \\ M'_T = \frac{M_T}{T_0 A h}, T' = \frac{T}{T_0}, c_{11} = \rho c_1^2. \end{aligned} \quad (28)$$

Using DQ as in equation (28) in equations (26) and (27), and then suppressing primes yields

$$\left[\nabla^4 + \delta_1 \frac{\partial^2}{\partial t^2} \right] w + \delta_2 \nabla^2 M_T = -P \delta_\varepsilon(x) \delta_\mu(y) e^{i\omega t}, \quad (29)$$

$$\begin{aligned} & \left(K_1^* + K_1 \frac{c_1}{L} \frac{\partial}{\partial t} \right) \nabla^2 T + \left(K_3^* + K_3 \frac{c_1}{L} \frac{\partial}{\partial t} \right) \frac{\partial^2 T}{\partial z^2} \\ & = \left(1 + \sum_{r=1}^N \frac{\chi^r}{r!} D_\chi^r \right) \left(\delta_3 \frac{\partial^2}{\partial t^2} (-2z \nabla^2 w) + \delta_4 \ddot{T} \right), \end{aligned} \tag{30}$$

where

$$\delta_1 = \frac{12L^2}{h^2}, \delta_2 = \frac{T_0 L}{h c_{11}}, \delta_3 = c_1^2 \beta_1^2, \delta_4 = \rho C_E c_1^2.$$

To find the solution to the problem, we can express the time-harmonic behavior as follows:

$$[w(x, y, t), T(x, y, z, t)] = [\bar{w}(x, y), \bar{T}(x, y, z)] e^{i\omega t}. \tag{31}$$

As a result,

$$M_T(x, y, t) = e^{i\omega t} \beta_1 \int_{-\frac{h}{2}}^{\frac{h}{2}} \bar{T}(x, y, z) z dz = \bar{M}_T(x, y, t) e^{i\omega t}. \tag{32}$$

Using equation (31) in (29) and (30) we have

$$[\nabla^4 - \delta_1 \omega^2] \bar{w} + \delta_2 \nabla^2 \bar{M}_T = -P \delta_\varepsilon(x) \delta_\mu(y), \tag{33}$$

$$\begin{aligned} & \left[\left(K_1^* + K_1 \frac{c_1}{L} i\omega \right) \nabla^2 + \left(1 + \sum_{r=1}^N \frac{\chi^r}{r!} G^r \right) \delta_4 \omega^2 \right] \bar{T} + \left(K_3^* + K_3 \frac{c_1}{L} i\omega \right) \frac{\partial^2 \bar{T}}{\partial z^2} \\ & - 2z \delta_3 \left(1 + \sum_{r=1}^N \frac{\chi^r}{r!} G^r \right) \omega^2 \nabla^2 \bar{w} = 0, \end{aligned} \tag{34}$$

where $G^r = (i\omega)^{r-1} \left[(1 - e^{-i\omega\chi}) \left(1 - \frac{2\beta}{\chi i\omega} - \frac{2\alpha^2}{\chi^2 \omega^2} \right) - \left(\alpha^2 - 2\beta + \frac{2\alpha^2}{\chi i\omega} \right) e^{-i\omega\chi} \right]$.

3.2 Thermal field in the thickness direction

It can be assumed that the TRP's thermal gradient along the x and y directions is very small as compared to its thickness,

$$\left(\frac{\partial^2}{\partial x^2} + \frac{\partial^2}{\partial y^2} \right) \bar{T} \ll \frac{\partial^2 \bar{T}}{\partial z^2}. \tag{35}$$

As a result,

$$\frac{\partial^2 \bar{T}}{\partial z^2} + p^2 \bar{T} = \delta_5 z \nabla^2 \bar{w}, \tag{36}$$

where

$$p = \omega \sqrt{\frac{\left(1 + \sum_{r=1}^N \frac{\chi^r}{r!} G^r \right) \rho C_E c_1^2}{\left(K_3^* + K_3 \frac{c_1}{L} i\omega \right)}}, \delta_5 = \frac{2\delta_3 \left(1 + \sum_{r=1}^N \frac{\chi^r}{r!} G^r \right) \omega^2}{\left(K_3^* + K_3 \frac{c_1}{L} i\omega \right)}.$$

In our scenario, it is assumed that no heat flows between the upper and lower surfaces of the TRP

$$\frac{\partial \bar{T}}{\partial z} = 0 \text{ at } z = \pm \frac{h}{2}. \quad (37)$$

As a result, the temperature distribution is given by

$$\bar{T} = \frac{2\beta_1^2}{\rho C_E} \left(z - \frac{\sin pz}{p \cos \frac{ph}{2}} \right) \nabla^2 \bar{w}. \quad (38)$$

Using (38) in (23) yields

$$\bar{M}_T = \frac{\beta_1^3 h^3}{6\rho C_E} (1 + f(p)) \nabla^2 \bar{w}, \quad (39)$$

where

$$f(p) = \frac{24}{p^3 h^3} \left(\frac{ph}{2} - \tan \frac{ph}{2} \right).$$

Now, applying equation (39) to equation (33) yields

$$\nabla^4 \bar{w} - \eta^4 \bar{w} = \epsilon_2, \quad (40)$$

$$\text{where } \eta^4 = \frac{\delta_1 \omega^2}{(1 + \epsilon_1 (1 + f(p)))}, \epsilon_1 = \delta_2 \frac{\beta_1 h^3}{12\rho C_E}, \epsilon_2 = \frac{-P \delta_\epsilon(x) \delta_\mu(y)}{(1 + \epsilon_1 (1 + f(p)))}. \quad (41)$$

3.3 Initial conditions

The initial conditions for an undeformed and homogeneous plate, at a uniform temperature T_0 and without rotation are considered as follows:

$$w(x, y, t)|_{t=0} = \frac{\partial w(x, y, t)}{\partial t} \Big|_{t=0} = 0, \quad T(x, y, t)|_{t=0} = \frac{\partial T(x, y, z, t)}{\partial t} \Big|_{t=0} = 0. \quad (42)$$

3.4 Mechanical boundary conditions

It is considered that the TRP ends are simply supported. Therefore, for simply supported edges $x = 0, a, y = 0, b$, the bending moment and deflection must be zero

$$w(x, y, t)|_{x=0,a} = M_{xx}|_{x=0,a} = 0, \quad w(x, y, t)|_{y=0,b} = M_{yy}|_{y=0,b} = 0, \quad (43)$$

$$M_T(x, y, t)|_{x=0,a, y=0,b} = 0, \quad (43)$$

$$M_{xx}|_{x=0,a} = \left[-c_{11} \left(I \frac{\partial^2 w}{\partial x^2} \right) - c_{12} \left(I \frac{\partial^2 w}{\partial y^2} \right) - M_T \right]_{x=0,a} = 0. \quad (44)$$

Subsequently $w(x, y, t) = 0$ along the edge $x = 0, a$, all the derivatives of w w.r.t. y are also zero. Therefore,

$$\frac{\partial w(x, y, t)}{\partial y} \Big|_{x=0,a} = 0, \quad \frac{\partial^2 w(x, y, t)}{\partial y^2} \Big|_{x=0,a} = 0. \quad (45)$$

If we use (45) in $M_{xx}|_{x=0,a} = 0$ it yields

$$\frac{\partial^2 w}{\partial x^2} \Big|_{x=0,a} = 0. \tag{46}$$

Likewise, $M_{yy}|_{y=0,b} = 0$ infers

$$\frac{\partial^2 w}{\partial y^2} \Big|_{y=0,b} = 0. \tag{47}$$

3.5 Solution of vibration

As per Debnath and Bhatta (2007) “the double finite Fourier sine transform (DFST) of a function F on a domain over a rectangular region $0 \leq x \leq a, 0 \leq y \leq b$ as a function of f_s :

$$DF_{is}(f(x, y)) = f_s(m, n) = \int_0^a \int_0^b F(x, y) \sin\left(\frac{m\pi x}{a}\right) \sin\left(\frac{n\pi y}{b}\right) dy dx. \tag{48}$$

The inverse double Fourier sine transform of a function f_s will be:

$$DF_{is}^{-1}(f_s(m, n)) = f(x, y) = \left(\frac{4}{ab}\right) \sum_{m=1}^{\infty} \sum_{n=1}^{\infty} f_s(m, n) \sin\left(\frac{m\pi x}{a}\right) \sin\left(\frac{n\pi y}{b}\right). \tag{49}$$

Theorem 1: If a function F vanishes on the boundary of the rectangular region $0 \leq x \leq a, 0 \leq y \leq b$ then:

$$DF_{is} \left(\frac{\partial^2 F(x, y)}{\partial x^2} + \frac{\partial^2 F(x, y)}{\partial y^2} \right) = -\pi^2 \left(\frac{m^2}{a^2} + \frac{n^2}{b^2} \right) f_s(m, n). \tag{50}$$

With the help of Pasquel (2019) and Al-Khaled (2018) equation (46) can be solved using a DFST in the x and y directions defined by equations (52) and (53) as

$$\bar{w}(x, y) = \left(\frac{4}{ab}\right) \sum_{m=1}^{\infty} \sum_{n=1}^{\infty} \bar{w}_s(m, n) \sin\left(\frac{m\pi}{a}x\right) \sin\left(\frac{n\pi}{b}y\right), \tag{51}$$

where m is the wavenumber along x and n along y directions.

Equation (42) with the help of equation (55) yields the value of $\bar{w}_s(m, n)$ as

$$\bar{w}_s(m, n) = \frac{-P \sin\left(\frac{m\pi \epsilon}{a}\right) \sin\left(\frac{n\pi \mu}{b}\right)}{\delta_6}, \tag{52}$$

where $\delta_6 = (1 + \epsilon_1 (1 + f(p))) \left\{ \left(\frac{m^2 \pi^2}{a^2} + \frac{n^2 \pi^2}{b^2} \right)^2 - \eta^4 \right\}$.

As a result, the expression for the TRP’s lateral deflection, temperature distribution, and the thermal moment is given by

$$w(x, y, t) = \left(\frac{4}{ab}\right) \sum_{m=1, n=1}^{\infty} \bar{w}_s(m, n) \sin\left(\frac{m\pi}{a}x\right) \sin\left(\frac{n\pi}{b}y\right) e^{i\omega_{mn}t}, \tag{53}$$

$$\begin{aligned}
 T(x, y, z, t) = & -\frac{\beta_1^2}{\rho C_E} \left(\frac{8}{ab}\right) \left(z - \frac{\sin pz}{p \cos \frac{ph}{2}}\right) \sum_{m=1, n=1}^{\infty} \left(\frac{m^2 \pi^2}{a^2} + \frac{n^2 \pi^2}{b^2}\right) \\
 & \times \bar{w}_s(m, n) \sin\left(\frac{m\pi}{a}x\right) \sin\left(\frac{n\pi}{b}y\right) e^{i\omega_{mn}t}, \quad (54)
 \end{aligned}$$

$$\begin{aligned}
 M_T(x, y, t) = & \frac{\beta_1^3 h^3}{3\rho C_E} \left(\frac{2}{ab}\right) (1 + f(\omega)) \sum_{m=1, n=1}^{\infty} \left(\frac{m^2 \pi^2}{a^2} + \frac{n^2 \pi^2}{b^2}\right) \\
 & \times \bar{w}_s(m, n) \sin\left(\frac{m\pi}{a}x\right) \sin\left(\frac{n\pi}{b}y\right) e^{i\omega_{mn}t}. \quad (55)
 \end{aligned}$$

3.6 Resonance conditions

Equation (41) provides the harmonic vibration frequency ω_{mn} of a Kirchhoff TRP as

$$\omega_{mn} = \omega_0 \left[1 + \frac{\epsilon_1}{2} (1 + f(p_0))\right], \quad (56)$$

$$\text{where } \epsilon_1 \ll 1, \omega_0 = \frac{h}{2\sqrt{3}L} \left(\frac{m^2 \pi^2}{a^2} + \frac{n^2 \pi^2}{b^2}\right), p_0 = \omega_0 \sqrt{\frac{(1 + G^r) \rho C_E c_1^2}{(K_3^* + K_3 \frac{c_1}{L} i \omega_0)}}, \quad (57)$$

$$n, m = 1, 2, 3, 4, \dots$$

The expression of thermoelastic damping is written as

$$Q^{-1} = 2 \left| \frac{\omega_{mn}^I}{\omega_{mn}^R} \right|, \quad (58)$$

where ω_{mn}^R and ω_{mn}^I are the real and imaginary parts of frequency ω_{mn} . The frequency shift because of thermal variations is written as:

$$\omega_S = \left| \frac{\omega_{mn}^R - \omega_0}{\omega_0} \right|. \quad (59)$$

4 Numerical results and discussion

To show our theoretical results and the effect of MDD, physical data of copper material is taken from Dhaliwal and Singh (1980) for numerical calculation

$$\begin{aligned}
 c_{11} &= 3.07 \times 10^{11} \text{ N m}^{-2}, & c_{12} &= 1.650 \times 10^{11} \text{ N m}^{-2}, \\
 c_{13} &= 1.027 \times 10^{10} \text{ N m}^{-2}, & c_{33} &= 3.581 \times 10^{11} \text{ N m}^{-2}, \\
 c_{44} &= 1.510 \times 10^{11} \text{ N m}^{-2}, & C_E &= 4.27 \times 10^2 \text{ J kg}^{-1} \text{ K}^{-1}, \\
 \beta_1 &= 7.04 \times 10^6 \text{ N m}^{-2} \text{ K}^{-1}, & \beta_3 &= 6.90 \times 10^6 \text{ N m}^{-2} \text{ K}^{-1}, \\
 K_1 &= 0.690 \times 10^2 \text{ W m}^{-1} \text{ K}^{-1}, & K_3 &= 0.690 \times 10^2 \text{ W m}^{-1} \text{ K}^{-1}, \\
 K_1^* &= 0.02 \times 10^2 \text{ N s}^{-2} \text{ K}^{-1}, & K_3^* &= 0.04 \times 10^2 \text{ N s}^{-2} \text{ deg}^{-1},
 \end{aligned}$$

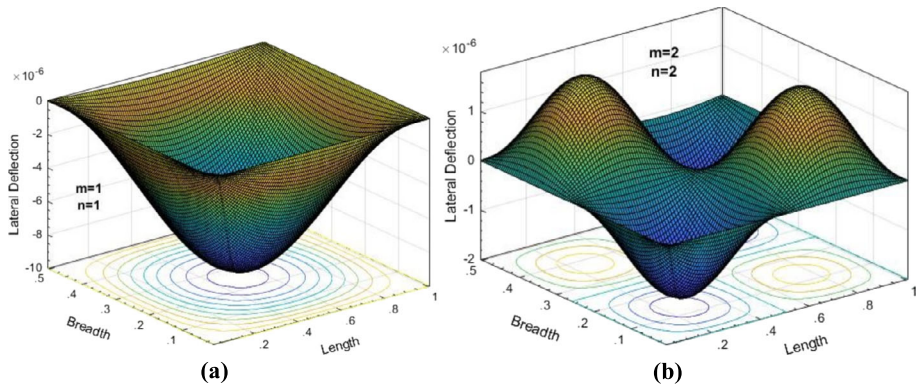


Fig. 2 (a and b). Deviation of Dimensionless Lateral Deflection w with MDD

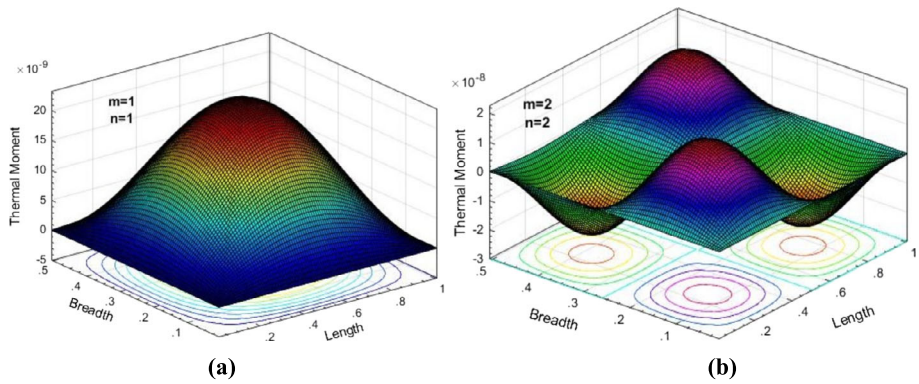


Fig. 3 (a and b). Deviation of Dimensionless Thermal Moment M_T with the length of the thin plate

$$\frac{L}{h} = 10, \quad \frac{b}{h} = 0.5, \quad \rho = 8.836 \times 10^3 \text{ kg m}^{-3}.$$

Figures 2(a and b) demonstrate the deviation in the dimensionless lateral deflection w w.r.t length and breadth of the thin plate with different mode numbers ($n = 1, m = 1$) and mode numbers ($n = 2, m = 2$) and the MDD kernel function value $\left[1 + \frac{(\xi-t)}{\chi}\right]^2$ when $\alpha = 1, \beta = 1$, respectively. It is observed in Fig. 2(a) that at the boundary of the plate the deflection in the lateral direction is zero and we have the maximum deflection at the center of the plate. Moreover, as the value of the mode number increases, as shown in Fig. 2(b), there is a corresponding change in the lateral deflection. At the boundary of the plate the deflection is zero, hence, it satisfies the boundary condition.

Figures 3(a and b) show the deviation of dimensionless thermal moment M_T w.r.t length and breadth of the thin plate with different mode numbers ($n = 1, m = 1$) and mode numbers ($n = 2, m = 2$) and the MDD kernel function value $\left[1 + \frac{(\xi-t)}{\chi}\right]^2$ when $\alpha = 1, \beta = 1$, respectively. It is observed in Fig. 3(a) that at the boundary of the plate the thermal moment is zero and we have the maximum variation at the center of the plate. The variation in the thermal moment shows the opposite behavior from the lateral deflection. Moreover, as the

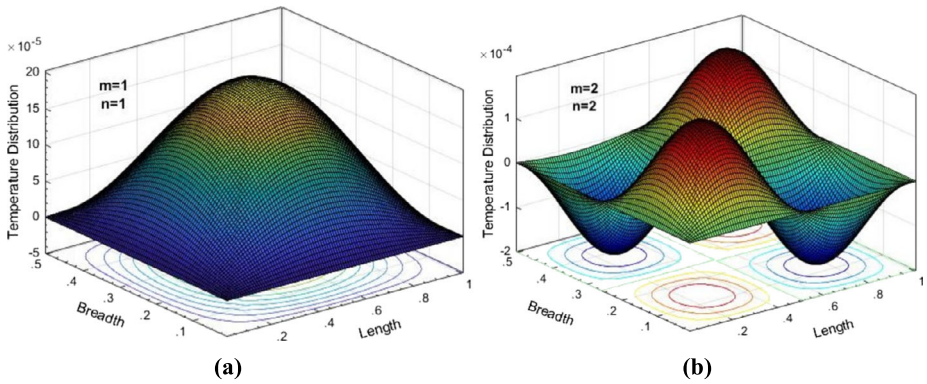


Fig. 4 (a and b). Deviation of Dimensionless Temperature Distribution with MDD

value of the mode number increases, as shown in Fig. 3(b), there is a corresponding change in the thermal moment. At the boundary of the plate the thermal moment is zero, hence, it satisfies the boundary condition.

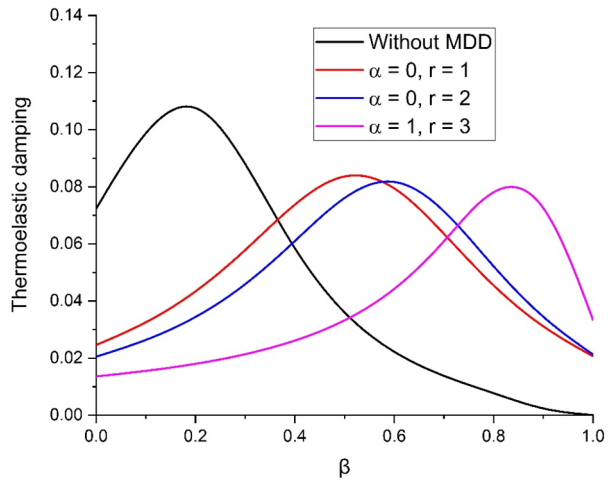
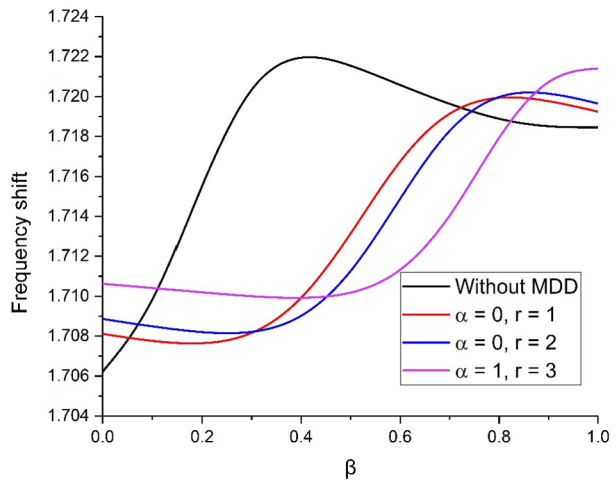
Figures 4(a and b) display the deviation of the dimensionless temperature distribution w.r.t length and breadth of the thin plate with different mode numbers ($n = 1, m = 1$) and mode numbers ($n = 2, m = 2$), and the MDD kernel function value $\left[1 + \frac{(\xi-t)}{\chi}\right]^2$ when $\alpha = 1$, $\beta = 1$, respectively. It is observed in Fig. 4(a) that at the boundary of the plate the temperature distribution is zero and we have the maximum variation at the center of the plate. The variation in the temperature distribution shows the opposite behavior from the lateral deflection. Moreover, as the value of the mode number increases, as shown in Fig. 3(b), there is a corresponding change in the temperature distribution. At the boundary of the plate the temperature distribution is zero, hence, it satisfies the boundary condition.

Figure 5 displays the variation in dimensionless thermoelastic damping with the change in the values of α and β the parameters of the kernel function of the MDD with mode numbers ($n = 2, m = 2$). The curves clearly illustrate that the kernel function influences the thermoelastic damping. Without the MDD, the thermoelastic damping is sharply decreased, whereas, it is different in the case with the higher-order parameter of the MDD. As the value of the higher-order parameter of the MDD increases, there is shift in the peak of the thermoelastic damping.

Figure 6 displays the variation in the dimensionless frequency shift with the change in the values of α and β the parameters of the kernel function of the MDD with mode numbers ($n = 2, m = 2$). The curves clearly illustrate that the kernel function influences the frequency shift. Without the MDD, the thermoelastic damping is sharply decreased, whereas it is different in the case with the higher-order parameter of the MDD. As the value of the higher-order parameter of the MDD increases, there is a shift in the graphs of the frequency shift.

5 Conclusions

The purpose of this study was to discuss higher-order memory-dependent derivatives with a delay-time parameter. Based on Taylor-series expansions to Fourier's law for higher-order MDD, a thermomechanical model is proposed for predicting the thermomechanical response of a rectangular transversely isotropic thermoelastic plate under a concentrated

Fig. 5 Variation of dimensionless thermoelastic damping

Fig. 6 Variation of dimensionless Frequency Shift


time-harmonic load. This model can be used to obtain different cases for many thermoelasticity models with and without memory dependence. The study and discussion were conducted on solutions based on a higher-order MDD kernel function. Based on the results obtained, the following conclusions can be drawn:

- A thin plate closed-form mathematical model is developed with Kirchhoff–Love plate theory and MDD. This study not only considered the size effect but also studied the memory, mechanical, and thermal-field effects.
- It has been observed that with the usage of higher-order MDD in the heat-conduction equation, the frequency shift and thermoelastic damping is predicted to be low, contrary to the heat-conduction equation without MDD. This infers that the memory-dependent derivatives can reduce damping and frequency shifts and improve MEMS/NEMS quality.
- The MDD theory is used to study and illustrate lateral deflections, thermal moments, and temperature distributions, and it is seen that the MDDs have a major effect on all the parameters of the thin plate.

Author contributions Iqbal Kaur: Conceptualization; Methodology; design; draft manuscript preparation; reviewed the results and approved the final version of the manuscript. Kulvinder Singh: Formal analysis and investigation; interpretation of results; Validation ; final manuscript preparation;

Declarations

Competing interests The authors declare no competing interests.

References

- Abouelregal, A.E.: An advanced model of thermoelasticity with higher-order memory-dependent derivatives and dual time-delay factors. *Waves Random Complex Media* **32**, 2918–2939 (2022). <https://doi.org/10.1080/17455030.2020.1871110>
- Abouelregal, A.E., Civalek, Ö., Oztop, H.F.: Higher-order time-differential heat transfer model with three-phase lag including memory-dependent derivatives. *Int. Commun. Heat Mass Transf.* **128**, 105649 (2021b). <https://doi.org/10.1016/j.icheatmasstransfer.2021.105649>
- Abouelregal, A.E., Moustapha, M.V., Nofal, T.A., Rashid, S., Ahmad, H.: Generalized thermoelasticity based on higher-order memory-dependent derivative with time delay. *Results Phys.* **20**, 103705 (2021a). <https://doi.org/10.1016/j.rinp.2020.103705>
- Al-Khaled, K.: Finite Fourier transform for solving potential and steady-state temperature problems. *Adv. Differ. Equ.* **2018**, 98 (2018). <https://doi.org/10.1186/s13662-018-1552-8>
- Alzahrani, F., Hobiny, A., Abbas, I., Marin, M.: An eigenvalues approach for a two-dimensional porous medium based upon weak, normal and strong thermal conductivities. *Symmetry* **12**, 848 (2020). <https://doi.org/10.3390/sym12050848>
- Amabili, M.: Theory and experiments for large-amplitude vibrations of rectangular plates with geometric imperfections. *J. Sound Vib.* **291**, 539–565 (2006). <https://doi.org/10.1016/j.jsv.2005.06.007>
- Amabili, M.: *Nonlinear Vibrations and Stability of Shells and Plates*. Cambridge University Press, Cambridge (2008). <https://doi.org/10.1017/CBO9780511619694>
- Bachher, M.: Plane harmonic waves in thermoelastic materials with a memory-dependent derivative. *J. Appl. Mech. Tech. Phys.* **60**, 123–131 (2019). <https://doi.org/10.1134/S0021894419010152>
- Beidouri, Z., Benamar, R., El Kadiri, M.: Geometrically non-linear transverse vibrations of C–S–S and C–S–C–S rectangular plates. *Int. J. Non-Linear Mech.* **41**, 57–77 (2006). <https://doi.org/10.1016/j.ijnonlinmec.2005.06.002>
- Debnath, L., Bhatta, D.: *Transforms and Integral Transforms*. Chapman & Hall, London (2007)
- Dhaliwal, R.S., Singh, A.: *Dynamic Coupled Thermoelasticity*. Hindustan Publication Corporation, New Delhi (1980)
- El Kadiri, M., Benamar, R., White, R.G.: Improvement of the semi-analytical method, for determining the geometrically non-linear response of thin straight structures. Part i: application to clamped–clamped and simply supported–clamped beams. *J. Sound Vib.* **249**, 263–305 (2002). <https://doi.org/10.1006/jsvi.2001.3808>
- Ezzat, M.A., El-Karamany, A.S., El-Bary, A.A.: Generalized thermo-viscoelasticity with memory-dependent derivatives. *Int. J. Mech. Sci.* **89**, 470–475 (2014). <https://doi.org/10.1016/j.ijmecsci.2014.10.006>
- Ezzat, M.A., El-Karamany, A.S., El-Bary, A.A.: A novel magneto-thermoelasticity theory with memory-dependent derivative. *J. Electromagn. Waves Appl.* **29**, 1018–1031 (2015). <https://doi.org/10.1080/09205071.2015.1027795>
- Ezzat, M.A., El-Karamany, A.S., El-Bary, A.A.: Generalized thermoelasticity with memory-dependent derivatives involving two temperatures. *Mech. Adv. Mat. Struct.* **23**, 545–553 (2016). <https://doi.org/10.1080/15376494.2015.1007189>
- Ezzat, M.A., El Karamany, A.S., El-Bary, A.A.: Thermoelastic viscoelastic materials with memory-dependent derivative. *Smart Struct. Syst.* **19**, 539–551 (2017). <https://doi.org/10.12989/sss.2017.19.5.539>
- Green, A.E., Naghdi, P.M.: On undamped heat waves in an elastic solid. *J. Therm. Stresses* **15**, 253–264 (1992). <https://doi.org/10.1080/01495739208946136>
- Gupta, S., Das, S., Dutta, R., Verma, A.K.: Higher-order fractional and memory response in nonlocal double poro-magneto-thermoelastic medium with temperature-dependent properties excited by laser pulse. *J. Ocean Eng. Sci.* (2022). <https://doi.org/10.1016/j.joes.2022.04.013>
- Kaur, I., Singh, K.: Fractional order strain analysis in thick circular plate subjected to hyperbolic two temperature. *Partial Differ. Equ. Appl. Math.* **4**, 100130 (2021a). <https://doi.org/10.1016/J.PADIFF.2021.100130>

- Kaur, I., Singh, K.: Thermoelastic damping in a thin circular transversely isotropic Kirchhoff–Love plate due to GN theory of type III. *Arch. Appl. Mech.* (2021b). <https://doi.org/10.1007/s00419-020-01874-1>
- Kaur, I., Singh, K.: Effect of memory dependent derivative and variable thermal conductivity in cantilever nano-beam with forced transverse vibrations. *Forces Mech.* **5**, 100043 (2021). <https://doi.org/10.1016/j.finmec.2021.100043>
- Kaur, I., Singh, K.: Functionally graded nonlocal thermoelastic nanobeam with memory-dependent derivatives. *SN Appl. Sci.* **4**, 329 (2022). <https://doi.org/10.1007/s42452-022-05212-8>
- Kaur, I., Singh, K.: An investigation on responses of thermoelastic interactions of transversely isotropic thick circular plate due to ring load with memory-dependent derivatives. *SN Appl. Sci.* **5**, 109 (2023). <https://doi.org/10.1007/s42452-023-05324-9>
- Kaur, I., Lata, P., Singh, K.: Forced flexural vibrations in a thin nonlocal rectangular plate with Kirchhoff's thin plate theory. *Int. J. Struct. Stab. Dyn.* **20**, 2050107 (2020). <https://doi.org/10.1142/S0219455420501072>
- Kaur, I., Lata, P., Singh, K.: Memory-dependent derivative approach on magneto-thermoelastic transversely isotropic medium with two temperatures. *Int. J. Mech. Mater. Eng.* **15**, 10 (2020). <https://doi.org/10.1186/s40712-020-00122-2>
- Kaur, I., Lata, P., Singh, K.: Effect of memory dependent derivative on forced transverse vibrations in transversely isotropic thermoelastic cantilever nano-beam with two temperature. *Appl. Math. Model.* **88**, 83–105 (2020). <https://doi.org/10.1016/j.apm.2020.06.045>
- Kaur, I., Lata, P., Singh, K.: Reflection of plane harmonic wave in rotating media with fractional order heat transfer and two temperature. *Partial Differ. Equ. Appl. Math.* **4**, 100049 (2021). <https://doi.org/10.1016/j.padiff.2021.100049>
- Lata, P., Kaur, I., Singh, K.: Deformation in transversely isotropic thermoelastic thin circular plate due to multi-dual-phase-lag heat transfer and time-harmonic sources. *Arab J. Basic Appl. Sci.* **27**, 259–269 (2020). <https://doi.org/10.1080/25765299.2020.1781328>
- Love, A.E.H.: The small free vibrations and deformation of a thin elastic shell. *Philos. Trans. R. Soc. Lond.* **179**, 491–546 (1888). <https://doi.org/10.1098/rsta.1888.0016>
- Majid, A., Abdeddine, E., Zarbane, K., Beidouri, Z.: Geometrically nonlinear forced transverse vibrations of C-S-C-S rectangular plate: numerical and experimental investigations. *J. Appl. Nonlinear Dyn.* **10**, 739–757 (2021). <https://doi.org/10.5890/JAND.2021.12.012>
- Marin, M., Agarwal, R.P., Mahmoud, S.R.: Modeling a microstretch thermoelastic body with two temperatures. *Abstr. Appl. Anal.* **2013**, 583464, 1–7 (2013). <https://doi.org/10.1155/2013/583464>
- Pasquel, F.: Double finite Fourier sine transform and computer simulation for biharmonic equation of plate deflection. *Eur. Int. J. Sci. Technol.* **8** 59–64 (2019)
- Rao, S.S.: *Vibration of Continuous Systems*. Wiley, New York (2007). <https://doi.org/10.1002/9780470117866>
- Sur, A., Kanoria, M.: Modeling of memory-dependent derivative in a fibre-reinforced plate. *Thin-Walled Struct.* **126**, 85–93 (2018). <https://doi.org/10.1016/j.tws.2017.05.005>
- Trivedi, N., Das, S., Craciun, E.-M.: The mathematical study of an edge crack in two different specified models under time-harmonic wave disturbance. *Mech. Compos. Mater.* **58**, 1–14 (2022). <https://doi.org/10.1007/s11029-022-10007-4>
- Ventsel, E., Krauthammer, T., Carrera, E.: Thin plates and shells: theory, analysis, and applications. *Appl. Mech. Rev.* **55**, B72–B73 (2002). <https://doi.org/10.1115/1.1483356>
- Wang, J.-L., Li, H.-F.: Surpassing the fractional derivative: concept of the memory-dependent derivative. *Comput. Math. Appl.* **62**, 1562–1567 (2011). <https://doi.org/10.1016/j.camwa.2011.04.028>
- Yu, Y.-J., Hu, W., Tian, X.-G.: A novel generalized thermoelasticity model based on memory-dependent derivative. *Int. J. Eng. Sci.* **81**, 123–134 (2014). <https://doi.org/10.1016/j.ijengsci.2014.04.014>

Publisher's Note Springer Nature remains neutral with regard to jurisdictional claims in published maps and institutional affiliations.

Springer Nature or its licensor (e.g. a society or other partner) holds exclusive rights to this article under a publishing agreement with the author(s) or other rightsholder(s); author self-archiving of the accepted manuscript version of this article is solely governed by the terms of such publishing agreement and applicable law.